Resonant ion-pair formation in electron collisions with rovibrationally cold H_3^+

S. Kalhori, R. Thomas, A. Al-Khalili, A. Ehlerding, F. Hellberg, A. Neau, and M. Larsson*
Department of Physics, Stockholm University, AlbaNova University Centre, S-106 91 Stockholm, Sweden

Å. Larson†
Department of Physics, The Royal Institute of Technology, AlbaNova University Centre, S-106 91 Stockholm, Sweden

A. J. Huneycutt and B. J. McCall
Department of Chemistry, University of California at Berkeley, Berkeley, California 94720, USA

N. Djurić‡ and G. H. Dunn
JILA, University of Colorado and National Institute of Standards and Technology, Boulder, Colorado 80309, USA

J. Semaniak and O. Novotny
Institute of Physics, Świętokrzyska Academy, 25 406 Kielce, Poland

A. Paál and F. Österdahl
Manne Siegbahn Laboratory, Stockholm University, S-104 05 Stockholm, Sweden

A. E. Orel
Department of Applied Science, University of California, Davis, Davis, California 95616, USA
(Received 8 September 2003; published 26 February 2004)

Experimental and theoretical cross sections for the resonant ion-pair formation (RIP) in electron collisions with rovibrationally cold H_3^+ ions are presented. Absolute cross sections for the RIP process producing H^- ions are measured for center-of-mass energies between 2–20 eV using the CRYRING, heavy-ion storage ring. Theoretical cross sections are obtained using wave-packet propagation on both one- and two-dimensional models of relevant diabatic-potential energy surfaces and couplings of H_3^+ and H_3.

DOI: 10.1103/PhysRevA.69.022713 PACS number(s): 34.80.Ht, 33.15.Bh, 33.15.Dj, 82.20.Fd

I. INTRODUCTION

H_3^+, with three protons and two electrons, is the simplest stable triatomic molecular ion. It plays an important role in the interstellar chemistry [1,2]. As a proton donor it initiates networks of chain reactions [3] leading to creation of complex molecules in both diffuse and dense interstellar clouds, the latter known to contain star formation regions [4]. H_3^+ is produced in the interstellar medium in a sequence of reactions initiated by the ionization of molecular hydrogen via cosmic rays, which is followed by reaction of the resulting H_2^+ with H_2

$$H_2^+ + H_2 \rightarrow H_3^+ + H. \tag{1}$$

Due to its importance in interstellar and planetary plasmas, H_3^+ has attracted the attention of physicists for many decades. Both the kinetics of H_3^+ creation and its further reactions with neutrals are rather well understood [5,6] in these regions, and the most important loss mechanism of H_3^+ in diffuse clouds is dissociative recombination (DR). DR is a process in which a molecular ion captures an electron and stabilizes by dissociating into neutral fragments, for example,

$$H_3^+ + e^- \rightarrow H_3^{**} \rightarrow \begin{cases} H_2 + H \\ H + H + H \end{cases}. \tag{2}$$

As the most efficient way of destroying molecular ions in very cold plasmas, DR plays a key role in the chemistry of interstellar clouds and, as such, directly influences H_3^+ number densities measured in such clouds. This is the subject of a recent debate since observations of relatively high H_3^+ column densities, e.g., towards the star Cygnus OB No. 12 and the Galactic center [2], which is not supported by the rather high rate coefficient for the DR of H_3^+ at low e^- energies measured in storage ring experiments [7–13]. To complicate the issue, experimentalists using different methods to determine this rate coefficient report results that differ by about four orders of magnitude. For many years theory has also not been able to solve the problem unambiguously. Recently, significant progress was achieved when a full three-dimensional calculation was carried out that revealed the importance of Jahn-Teller coupling in the DR process of H_3^+ [14,15].

At higher collision energies of the order of a few eV, but still representative for rather cold plasma in which the mo-

*Corresponding author. Email address: ml@physto.se
†Present address: JILA and Department of Physics, University of Colorado, Boulder, Colorado 80309-0440, USA.
‡Present address: Jet Propulsion Laboratory, 4800 Oak Grove Drive, Pasadena, 91109 CA, USA.

lecular bond of H_3^+ can survive, the DR cross section reveals a broad resonance structure, the presence of which has been confirmed by many storage ring measurements [7–13]. In the same energy regime, another dissociation process involving the same intermediate states as in the DR process occurs. This process is called resonant ion-pair formation (RIP). Following the initial capture of the electron into the doubly excited neutral intermediate state, the process stabilizes through the formation of a charged ion pair. In the present study the total cross section for the following two RIP reaction channels has been measured

$$H_3^+ + e^- \rightarrow H_3^{**} \rightarrow \begin{cases} H^- + H_2^+ \\ H^- + H^+ + H. \end{cases} \quad (3)$$

The threshold energy E_{th} for these channels are determined to be 5.4 eV and 8.1 eV, respectively [16]. RIP is an important process in plasma processing generators, flames, and even the edge plasmas of Tokamaks.

Apart from its applicability, the study of the RIP process is of fundamental interest. It represents a unique possibility to investigate a few dissociation channels simultaneously with a well-defined collision energy and good statistical precision. In the case of DR, where the sharing of the dissociation flux over many asymptotic states yields different atomic or molecular products, the same task requires utilization of much more complicated experimental procedures and thus is limited to selected collision energies.

RIP data from studies on H_3^+ have previously been published in the literature. Peart *et al.* [17] used an inclined beams technique while Yousif *et al.* [18] and Larsson *et al.* [12] used merged beams techniques, the former in a single pass apparatus and the latter using the CRYRING heavy ion storage ring. Peart *et al.* [17] and Yousif *et al.* [18] report absolute cross-section data while Larsson *et al.* [12] report relative cross-sections data. It is clear from these results that the presence of excited H_3^+ ions in the beam can greatly influence the RIP process.

In the present paper we report absolute cross sections for the RIP of vibrationally and rotationally cold H_3^+ ions measured using the storage ring technique. For technical reasons, we are only able to detect the light negative product of the RIP process, i.e., H^-. Thus the total cross sections apply to the total of the dissociation channels in Eq. (3) above. The experimental results are compared with theoretical predictions. In the theoretical model, the dynamics of the system is studied using wave packets, propagating on electronically coupled diabatic potentials of H_3. This method has previously been used to calculate RIP cross sections in electron recombination with HeH^+ and HD^+ by Larson *et al.* [19,20].

II. EXPERIMENT

A. General

The merged beams technique using storage rings has been described in detail a number of times previously, see, for example, Refs. [21,22], and we touch only on salient features here. The experimental arrangement is shown schematically in Fig. 1. A circulating beam of ions of current I_i and velocity v_i is merged over a path length l with a colinear uniform beam of electrons of current I_e and velocity v_e and cross-sectional area πr^2. Collision products are formed at a rate dN/dt, and these products are separated from the main ion beam by the dipole magnetic field just after the merging region and detected there by an energy sensitive detector (SBD), referred to as the primary detector. The rate coefficient in the experiment, in terms of the collision cross section σ and relative velocity v, is given by

$$\langle \sigma v \rangle = \frac{dN}{dt} \frac{v_e v_i e^2 \pi r^2}{I_i I_e l}. \quad (4)$$

Thus, an experiment to measure the collision cross section requires the measurement or preknowledge of each of the quantities in Eq. (4). The path length l (commonly called the cooler length) and the electron beam cross-sectional area πr^2 have been characterized many times previously [22], and are well-established numbers for this experiment. The electron current, I_e, is measured in a conventional way using a Faraday cup collector. The ion current, I_i, is obtained for relative measurements by monitoring products formed by collisions of the ions with background gas in the ring using an auxiliary detector mounted at the end of one of the straight sections in the ring, i.e., the neutral particle monitor in Fig. 1. It is noted that the primary detector is also used for this purpose when the relative collision energy is below threshold for the RIP process, e.g., 2 eV. Since the background gas pressure is stable and the energy of the ions is constant, the time-dependent background count rate is a reliable monitor of the relative ion current. For absolute measurements, the ion current was measured with a sensitive current transformer at the same time as the signal from background processes. The magnetically separated fragments from the RIP process are detected using an SBD, whose output pulses are dependent on the energy deposited by a given particle, so that H^- ions can be easily discriminated from noise. There are, however, gas collision events producing H^-, and these must be subtracted after determining their number by measuring the ''signal'' below threshold for RIP as described above. By measuring the number of H^- ions formed in a given time, the signal rate *dN/dt* is thus determined.

B. Ions

One of the main aspects of the CRYRING, TSR, ASTRID, and other storage ring facilities is that in storing ions with infra-red active modes for a sufficient period of time before data acquisition, the ions decay into their vibrational ground states. Experiments at TSR have shown that with 2 s of storage time, the H_3^+ had relaxed into their ground vibrational state [11]. Although it was clear that H_3^+ had vibrationally relaxed, these results showed that the same was not true for the rotational energy. For the most part, the effects of rotational energy on the DR process had previously been neglected, being thought insignificant. However, these data from TSR [11] and a few very recent experiments con-

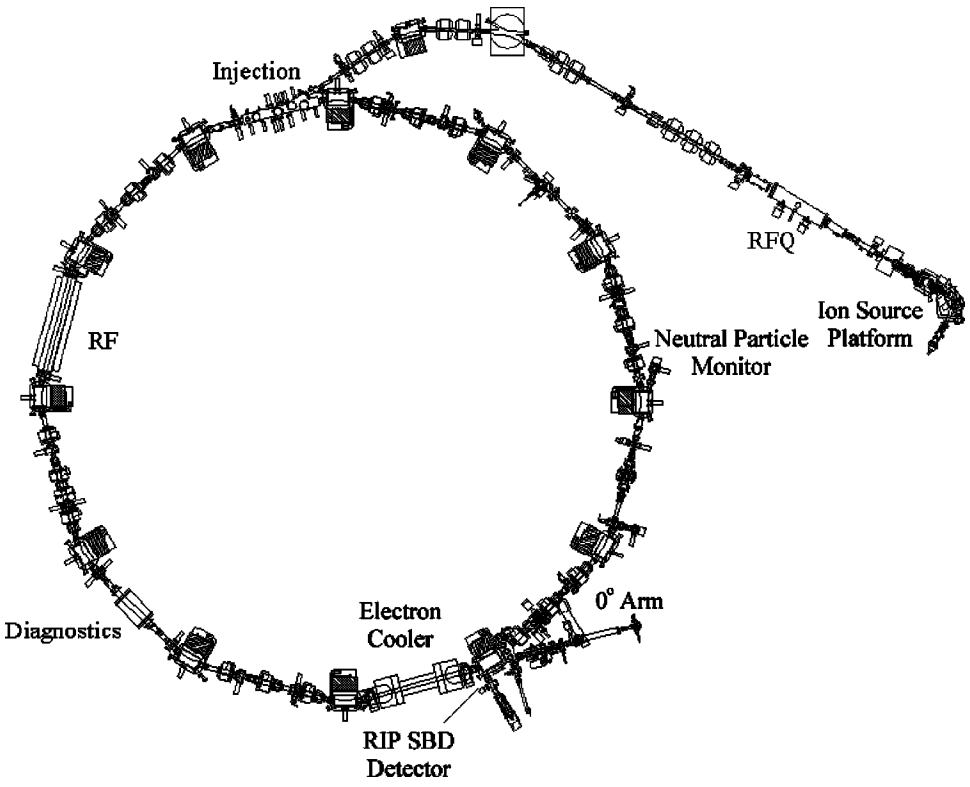

FIG. 1. Layout of the storage ring facility CRYRING. The ions are created in a supersonic expansion ion source, with a 90° separator magnet used for mass selection. The mass selected ions are accelerated by an rf quadrupole (RFQ) up to 300 keV/amu before being injected into the ring. Once injected, the ions are then accelerated to the required beam energy. In the ''electron cooler'' section the ions interact with electrons, and the negative fragments from the RIP process, together with background interactions, are detected by a moveable SBD located in the dipole chamber following the electron cooler. Monitoring the number of ions in the beam, required for absolute measurements, is achieved using an MCP detector, known as the neutral particle monitor, positioned at the end of one of the straight sections after the electron cooler.

ducted at CRYRING indicated that this approach was flawed and that the effect of rotational energy could be significant, especially at collision energies of a few meV [12,13]. To investigate the importance of the effects of rotation, a supersonic expansion ion source was developed and characterized, which could supply ions with a rotational temperature of only 20–60 K [13]. However, it is important to state that the source only delivered rotationally cold ions, and that the ions' vibrational energy was reduced by storage in CRYRING for a few seconds.

We measured the DR rate coefficient using this ion source [13], and these new data showed much clearer structure in the cross-section curve, structures which had only previously been suggested in an earlier measurement [12]. Since this source produced rotationally cold H_3^+ ions and the storage ring method produces vibrationally cold H_3^+, it was decided that while the source was in place there was a unique opportunity for also studying the RIP process under well-defined conditions. The H_3^+ ions, after mass selection, were injected into the ring. Then the rotationally cold ions were accelerated to 7.55 MeV. It is worth noting that in obtaining the DR data reported in Ref. [13], attempts to deliberately ''heat'' the ion beam before taking cross-section measurements did not lead to any significant differences in the data. These and other tests expanding on the results reported in Ref. [13] are discussed in a more detailed paper, which is in preparation [23]. It was therefore concluded that no significant heating of the ion-beam occurred during the experiment, and that the electrons in the interaction region always reacted with rotationally cold H_3^+ and that this situation should be no different for the RIP process studied here.

C. Electrons, collision energies, and data protocol

During each cycle the stored ion beam traveled through a monoenergetic and colinear electron beam. The electrons have an anisotropic Maxwell-Boltzmann distribution characterized by different longitudinal $T_{e\|}$ and transverse $T_{e\perp}$ temperatures

$$f(v)=\frac{m_e}{2\pi kT_{e\perp}}\left(\frac{m_e}{2\pi kT_{e\|}}\right)^{1/2}\exp\left(-\frac{m_e v_{e\perp}^2}{2kT_{e\perp}}-\frac{m_e v_{e\|}^2}{2kT_{e\|}}\right), \tag{5}$$

where k is the Boltzmann constant and m_e and v_e are the electron mass and velocity, respectively. For the electron beam in CRYRING, the longitudinal and transverse vector components of the electron velocity are given by $v_{e\|}$ and $v_{e\perp}$, respectively. The continuously renewed electron beam acts as a cooling medium for the circulating ion beam. Ef-

fective cooling is obtained when the average electron and ion velocities are matched. With each passage of the ions through the cold electron beam, heat is transferred from the ion beam to the electron beam. As a result, the random thermal motion of the ions is reduced. This leads to a reduction of the ion-beam diameter, down to about 1 mm, with a corresponding increase in the phase-space density. The electron beam of the cooler also serves as a source of electrons for the RIP process. The interaction energy (eV) in the center-of-mass (c.m.) frame, $E_{c.m.}(t)$, as a function of storage time t is given by

$$E_{c.m.}(t)=(\sqrt{E_{cath}(t)}-\sqrt{E_{cool}})^2. \tag{6}$$

Here E_{cool} corresponds to the electron energy (in Volts) in the laboratory frame of reference when the electron and ion velocities are matched. This matching condition has been accurately determined during the preceding measurement of the DR rate coefficient [13]. In the present experiment, $E_{c.m.}$ was varied with E_{cath} (in Volts), i.e., by changing the electron-cooler cathode voltage (CV) as a function of storage time, t. In this scheme CV is set to the optimum cooling condition for 3 s. In 2 ms, CV is ramped to provide a c.m. energy of 2 eV and is kept at this value for 1 s. Then the CV is quickly changed to give a collision energy of 20 eV. This value is held for 100 ms to allow time for the power supply to stabilize. Then, in 1 s, the CV is slowly ramped back down to a c.m energy of 2 eV and kept at this value for 1 s. Then the entire scheme is repeated in reverse. The main reason why the scan is reversed is to allow a check for any time-dependent effects on the RIP process. In order to have an absolute energy scale, several corrections are routinely applied, and detailed discussions of how these corrections are applied can be found elsewhere [24,25]. The most important correction which has to be applied to these data is due to the effect of the toroidal magnets at the front and back of the electron cooler. These magnets steer the electron beam into and out of the cooler and, as such, give rise to nonparallel merging of the electron and ion beams meaning that the collision energies in these regions are higher than those in the center of the electron cooler. The contribution of the events occurring in the toroidal section has been subtracted using the iterative procedure explained in detail in Ref. [26], using the latest data of the electron-cooler magnetic field [27].

D. Cross sections

Using the procedures outlined above and using the relative ion current obtained from the background gas monitors described, the relative rate coefficient was obtained for the range of collision energies 2–20 eV. The relative averaged cross section σ_{rel} is obtained from the measured rate coefficient after dividing it by the collision velocity v_d, which is equal to the absolute difference between average velocities of ions and electrons

$$\sigma_{rel}=\frac{\langle \sigma v \rangle}{v_d}. \tag{7}$$

In order to obtain absolute cross-section data, the RIP count rate at the specific collision energy of 11 eV was measured as a function of storage time simultaneously with the absolute ion-beam current. These absolute data were then corrected to account for the effects mentioned in the preceding section. The absolute uncertainty is calculated for the cross-section maximum only, obtained by considering both systematic and statistical effects in quadrature. At the maximum, the uncertainty is dominated by the systematic errors, arising from the ion, I_i, and electron, I_e, beam current measurements, $\approx 10\%$ and $\approx 5\%$, respectively, and the effective reaction length, $\approx 10\%$. The statistical uncertainty in the cross sections varies from 6% at the peak value to 40% at the threshold. The estimated absolute uncertainty at the maximum of the RIP cross section is about 15% at the 1σ level.

III. THEORETICAL METHOD

We have studied the wave-packet dynamics using a diabatic representation of the H_3 potentials. When the incoming electron is captured by H_3^+, a doubly excited state of H_3 is formed. According to electron scattering calculations by Orel and Kulander [28], there are four repulsive resonant states of H_3 lying in the energy region of 5–16 eV above the lowest vibrational level of H_3^+. In the C_{2v} geometry, two of these states have the symmetry $^2A_1$ and the other two have $^2B_2$ symmetry. Previous theoretical studies of these states showed that in the vicinity of the equilateral geometry of the ion, three of these states are interacting in a triple intersection [29]. The dominant configuration of one of the $^2A_1$ resonant states is $1a_1 2a_1^2$, which diabatically dissociates into the ion-pair limit $H_2^+ + H^-$ at infinity [30,32].

A. One-dimensional study

To simplify the problem, first a one-dimensional model of the potentials has been applied. Using this model, it will be possible for us to get a clear insight of the reaction dynamics, since the effects from the various couplings can easily be studied. We will start by discussing the different potentials and couplings that are relevant in the present study. The dynamics of H_3 is studied in C_{2v} symmetry, where $\theta=90°$ and $R=1.65a_0$ are kept fixed, while the distance z is varied (see Fig. 2). Here a diabatic representation of the potential-energy surfaces and couplings has been used for the wave-packet propagation. At small internuclear distances, $z<2.55a_0$, the doubly excited neutral states are situated above the ion potential. The potential-energy surfaces then cannot be calculated using standard quantum chemistry calculations. Instead the potential-energy surfaces and the corresponding autoionization widths Γ_i are calculated using a Complex-Kohn electron scattering variational method [28]. In order to study the interactions between the two resonances of $^2A_1$ symmetry, a series of restricted configuration-interaction (CI) calculations are carried out in the Franck-Condon region. In these calculations, the $1a_1$ orbital remains singly occupied and not more than one electron is excited to the virtual space. This eliminates the contributions from the background $1a_1^2 ka_1$ and $1a_1^2 kb_2$ states, which represent a free electron in the field of

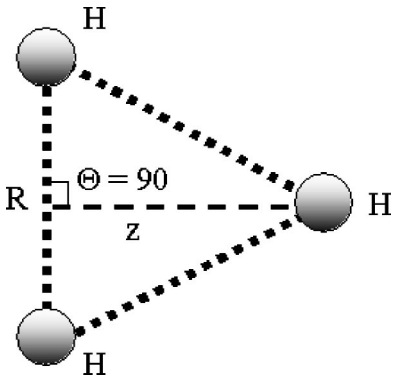

FIG. 2. The Jacobi coordinates used in the present calculation. In the one-dimensional study R and θ are kept fixed to $R=1.65a_0$ and $\theta=90°$, respectively, while z is varied. In the two-dimensional study, both R and z are varied, while $\theta=90°$.

the electron core. For further details on the approach used in these calculations, see [28,29]. From the CI coefficients of the electronic wave functions of the two $^2A_1$ resonances, it is clear that the two states change character through the avoided crossing at $R=1.65a_0$ and $z=1.4289a_0$. The electronic coupling between the diabatic resonant states is calculated using a two-by-two transformation of the adiabatic potentials with a rotational angle calculated from the CI coefficients of the ion-pair configuration [19,33]. As mentioned above, one of the $^2A_1$ resonant states will diabatically correlate with the ion-pair limit at infinity. The diabatic potential of this state is, at first, attractive as z is increased and therefore crosses the Rydberg state potentials of H_3 situated below the H_3^+ potential. The second $^2A_1$ resonant state will asymptotically correlate with one of the neutral fragment channels that is not measured in the present experiment. In order to obtain information about the diabatic neutral potentials below the ion potential of H_3^+, adiabatic potential energy curves of the 10 lowest Rydberg states of H_3 are calculated using the CI method. Again, using the CI coefficients, it is possible to identify the ion-pair configuration $1a_1 2a_1^2$ in the CI expansion of the electronic wave function of the Rydberg states. From this information, we could estimate where the diabatic ion-pair state is attractive and crosses the manifold of Rydberg state potentials. At larger z, when the ion-pair potential becomes repulsive again in energy, and crosses some of the Rydberg states once more, it was not possible to identify the ion-pair configuration and therefore we simply used the shape of the avoided crossings of the adiabatic potentials to estimate the corresponding diabatic potentials and couplings. For $z \geqslant 20a_0$ we assume that the Rydberg state potentials are constants and the ion-pair state can be approximated by a Coulomb potential, including the polarizability [31]. In the upper panel (a) of Fig. 3 the one-dimensional adiabatic potentials obtained from the CI calculation are shown. The corresponding diabatic potentials that are used in the wave-packet propagation are displayed in the lower panel (b) of Fig. 3. Note that the ground-state potential of H_3 is not included in either of these panels. It is situated much below the relevant Rydberg state potentials and will not couple to the ion-pair state. The ion potential of H_3^+ is

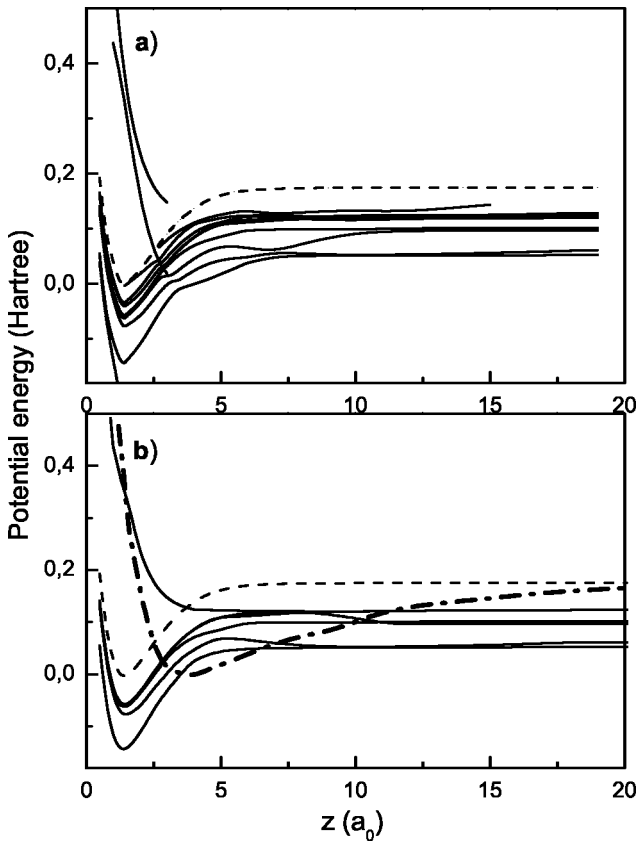

FIG. 3. (a) *Ab initio* calculated adiabatic potential-energy curves of H_3^+ (dashed curve) and H_3 (solid curves). The energy scale is relative to the lowest vibrational level of H_3^+. The neutral states situated above the ion (resonant states) are obtained from electron scattering calculations and the curves of the ion and the neutral (Rydberg) states situated below the ion are calculated using the configuration interaction method. (b) Diabatic potential-energy curves that are used in the one-dimensional model. The dashed curve is the ionic potential and the solid curves are the potentials of the neutral states. The thick dot-dash curve is the diabatic ion-pair state.

included in the figure with a dashed line. As can be seen in panel (b) of Fig. 3 the diabatic potential-energy curves of identical symmetry are allowed to cross and the electronic couplings between these states have to be estimated. As described above, the coupling between the two resonant states are obtained by the two-by-two transformation of the adiabatic potentials. However, we could not use this method to calculate the couplings between the resonant doubly excited states and the Rydberg states of H_3. Instead the couplings to the resonant states at small internuclear distances are estimated using a scaling of the autoionization widths [34]

$$C_{ij}(z)=\sqrt{\frac{\Gamma_i(z)}{2\pi}}[n_j^{eff}(z)]^{-3/2}, \tag{8}$$

where $n_j^{eff}(z)$ is the effective quantum number of Rydberg state j, calculated using the energy difference between the ion and Rydberg potentials. There are an infinite number of Rydberg states converging up to the ion. All these states will

couple to the resonant states at small internuclear distances. In order to assess the effects from these states an ''effective coupling'' was used for the highest Rydberg state included in the calculation [33]. At large internuclear distance where the ion-pair potential goes up and crosses some of the Rydberg state potentials again, the electronic couplings are estimated by half of the energy difference between the corresponding adiabatic potentials.

When two resonant states with the same electronic symmetry are close to each other, they will not only couple to each other directly, but they can also interact in second order via electronic coupling to the nonresonant scattering continuum. This is the case for the two $^2A_1$ resonant states present in this model. This type of interaction has previously been studied by Estrada *et al.* [35] and Hazi [36]. In the present study, the energies of the resonances in the Franck-Condon region (5–16 eV) is much larger than spacing between the vibrational levels of the ion and the ''local approximation'' can be applied. By neglecting the real part of the indirect coupling, we get the following simple expression for the interaction between the two resonant states via the continuum

$$W_{ij} = -i\pi\sqrt{\frac{\Gamma_i(z)}{2\pi}}\sqrt{\frac{\Gamma_j(z)}{2\pi}}. \tag{9}$$

Details on this coupling and the implications for DR are given in Royal *et al.* [37].

The wave packets are propagated using the one-dimensional diabatic potential-energy curves and couplings of H_3 described above. For the wave-packet propagation, seven states are included. These are the two resonant states described above, where one of them diabatically correlates with the ion-pair limit at infinity. There are also five Rydberg states included, where the one with the highest energy is the ''effective'' Rydberg state. The wave packets are propagated by solving numerically the time-dependent Schrödinger equation

$$i\frac{\partial}{\partial t}\mathbf{\Psi}(z,t) = \hat{\mathbf{H}}\mathbf{\Psi}(z,t) \tag{10}$$

by using the Crank-Nicholson method [38]. The Hamiltonian operator above becomes a nondiagonal, non-Hermitian, symmetric matrix where the diagonal elements contain the kinetic-energy operator and the potentials and the off-diagonal elements are the electronic couplings. It is assumed that when the electron has recombined with H_3^+, a superposition of the two doubly excited resonant states $^2A_1$ of H_3 is formed. The capture into the Rydberg states is neglected. This approximation is justified at the relevant electron collision energies (above 5 eV) where the nonadiabatic couplings between the Rydberg states and the ionization continuum can be neglected compared with the electronic coupling. Thus, at $t=0$ wave packets are initiated on the resonant states

$$\Psi_i(z,t=0) = \sqrt{\frac{\Gamma_i(z)}{2\pi}}\chi_{\nu=0}(z), \quad i=1,2. \tag{11}$$

The vibrational wave function $\chi_{\nu=0}(z)$ for the $\nu=0$ vibrational level in the ground state of H_3^+ is calculated using a finite difference method [39] to solve the time-independent Schrödinger equation for the one-dimensional ion potentials shown in Fig. 3. Before the wave packets on the resonant states reach the point where the resonant state potentials cross the ionic state potential, there is a probability that the electron is reemitted again, i.e., autoionization. The autoionization can be included in the local complex approximation, by using a complex potential of the ion-pair state

$$W_i(z) = V_i(z) - i\tfrac{1}{2}\Gamma_i(z). \tag{12}$$

The wave packets are then propagated out to the asymptotic region where the autoionization width has ceased and the electronic couplings between the neutral states are zero. In order to compare with the experiment we calculate the cross section of ion-pair formation by projecting the asymptotic wave packet on the ion-pair state onto the scattering wave functions. The cross section is given by

$$\sigma(E) = g\frac{2\pi^3}{E}\lim_{t\to\infty}|\langle\Phi_E|\Psi_1(t)\rangle|^2, \tag{13}$$

where $g=1$ is the multiplicity ratio of the ion plus free electron and the neutral ion-pair state. Since the ion-pair state has a long-range potential it is not possible to use plane waves as scattering wave functions. Instead the wave packet is projected on the energy-normalized eigenfunctions $\Phi_E(z)$ calculated using the finite differencing method on the ion-pair potential.

B. Two-dimensional study

When the doubly excited resonant states are formed by the electron recombination with H_3^+, the system can also dissociate into neutral fragments (DR). This process has previously been studied by Orel and Kulander [28]. From this theoretical study, the importance of including both C_{2v} degrees of freedom (R and z in Fig. 2) in the electron capture and dissociation dynamics became clear. These calculations showed that although in the Frank-Condon region the resonant states were steeply varying as both a function of z and R, scattering calculations in the C_s symmetry in this region showed the surface was almost flat as a function of θ. Therefore, the dissociation does not follow a single normal mode coordinate, but it is a reasonable approximation to ignore the spreading which takes place in angle during the rapid dissociation. The next step in the present study of ion-pair formation is thus to also include the second degree of freedom, which corresponds to variations of the H-H distance R in Fig. 2. In these calculations, the C_{2v} symmetry is always conserved and the angle θ is kept fixed to 90°. In the two-dimensional wave-packet propagation, the time propagation is performed with the Chebychev method [40], which proceeds by expanding the time evolution operator in a set of complex Chebyshev polynomials. For details see Ref. [41]. Again, the two diabatic resonant potential-energy surfaces of the states with $^2A_1$ symmetry, cross each other at the equi-

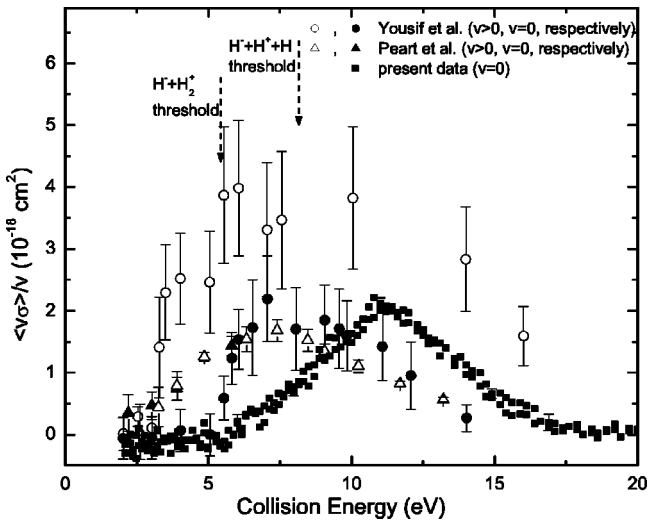

FIG. 4. Comparison of the RIP cross sections reported here (solid squares) with those obtained from earlier studies reported by Peart *et al.* [17] (triangles) and Yousif *et al.* [18] (circles). For Peart *et al.* [17] and Yousif *et al.* [18], the open and filled symbols represent data obtained under conditions where it is known that there are vibrationally excited ions present in the beam and where attempts were made to measure with only ground-state ions, respectively.

librium geometry of the H_3^+ ion. Both the direct and indirect coupling between these resonant states are included in the calculation. The direct couplings are calculated using the orthogonal transformation of the adiabatic potential-energy curves as described above in Sec. III A. Autoionization from the resonant states are again included by using complex potentials. In the wave-packet propagation, it is assumed that one of the resonant states diabatically dissociates to the ion-pair limit at infinity. In the present study no loss to the Rydberg states is included. Therefore, the present two-dimensional study will only yield an upper limit of the ion-pair cross section. A detailed study of the dynamics on the two-dimensional potential-energy surfaces of H_3, where also the couplings to the Rydberg states will be included, will be published in the future [42].

When the wave packets are propagated out to the asymptotic regions, the ion-pair wave packet is analyzed by projecting it onto the two-dimensional eigenfunctions $\Phi_E(R,z)$ to obtain the ion-pair cross section according to Eq. (13). Since coupling to the Rydberg states was not included, we distorted the resonance surfaces in the asymptotic region to become flat in z and R [28]. We therefore can analyze the wave packet by simply projecting onto plane waves in the two-dimensional space.

IV. RESULTS AND DISCUSSION

A. Experimental results

The measured cross section obtained for the production of H^- from the reaction of H_3^+ with electrons is plotted in Fig. 4 as solid squares. As mentioned in the analysis, for each injection cycle two RIP data sets were obtained, i.e., one for each of the CV ramping schemes. As expected, these data sets were found to be in agreement and were thus combined together and the cross section calculated as detailed in the experimental section. It can be seen that the overall shape of the curve is quite broad, peaking at a value of $\approx 2.3 \times 10^{-18}$ cm^2 at a collision energy of 11 eV. It is important to note that the peak shape for the data reported here, for rotationally and vibrationally cold ions, is essentially the same as was reported from the earlier experiment at CRYRING by Larsson *et al.* [12]. However, the position of the peak as well as the determined threshold have been found to be shifted by about 0.5 eV up with respect to this earlier study. At present the threshold energy agrees very well to that expected for the first of the two dissociation channels given in Eq. (3). The differences obtained in the earlier experiment were due to an incorrect determination of the electron trajectory in the toroidal regions.

Also plotted in Fig. 4 for comparison are the cross sections obtained by Peart *et al.* [17] and Yousif *et al.* [18] for the measurement of H^- arising from the two channels given in reaction (3). Both of these groups conducted two sets of experiments. The first were run with the ion source in such a way as to provide vibrationally excited, $\nu > 0$, ions. In the second set of experiments, they ran their ion sources at much higher pressures, which is known to lead to collisional quenching and, as such, provides a way to produce colder ions [18].

The magnitude of all three reported cross sections for vibrationally relaxed ions is the same within the experimental uncertainties. However, the structure of the cross sections is very different. The cross section obtained from the present experiment has a more symmetric shape, and is not as broad, as that reported by Peart *et al.* In addition, the threshold energies significantly differ by 2.5 eV. The cross section reported by Yousif *et al.* also differs greatly from that reported here; the energy dependence of the cross section in the threshold region is much sharper, though they report the same threshold energy as obtained in the present experiment. Finally, it can be seen that the peak position in the cross sections reported here is much higher, by 4 eV, than those reported by Peart *et al.* and Yousif *et al.*

The question has to be asked as to the source of the differences in these experiments. It is known that the storage ring technique allows for complete vibrational relaxation of the H_3^+ ions, independent of the creation method of the ions, as shown from the TSR experiment which produced H_3^+ ions with $T_{vib} = 2000$ K [11]. Thus, it would seem that the difference from these experiments probably derives from differences in the vibrational temperature of the ions in the experiments conducted by Yousif *et al.* and Peart *et al.*, though Yousif *et al.* felt that they had evidence that their ions were vibrationally cold. It is worth noting that Peart *et al.* concluded from their own results that they might not have been successful in their attempt to obtain cold ions, a conclusion also suggested by Yousif *et al.* in discussing the Peart *et al.* data.

In Fig. 5 the present RIP cross section data are plotted together with the DR cross-section data measured during the same experiment and which was reported in Ref. [13]. Both cross sections exhibit similar resonant structures with a

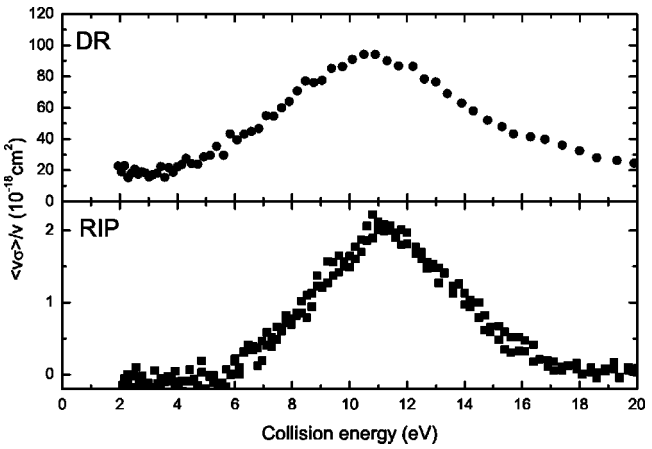

FIG. 5. Comparison of the RIP cross sections reported here (solid squares) with the DR cross sections reported by McCall *et al.* [13].

maximum at 11 eV. As can be seen, the magnitude of the RIP cross section is considerably smaller and reaches only 2% of that found for the DR cross section at its maximum. Moreover, the resonant structure of the RIP cross section is more narrow than the one seen in the DR data. As has been reported by Orel and Kulander [28], the observed resonant structure can be explained by electron capture into four doubly excited states, two of $^2A_1$ symmetry and two of $^2B_2$ symmetry. Each of them yield resonances which contribute to the observed peak in the DR cross section [28]. At energies below and around the threshold for the RIP process, the DR of H_3^+ is dominated by resonant capture to the intermediate $1\ ^2A_1$ and $1\ ^2B_2$ states. Production of H^- ions become energetically possible at collision energies of 5.4 eV, and proceeds via one of the $^2A_1$ states, with $1a_1 2a_1^2$ configuration, and dissociating to the $H^- + H_2^+$ limit at infinity. The rather small flux into this RIP dissociation channel, compared to the DR channel, suggests that most of the dissociation flux along this state potential is distributed over the manifold of Rydberg states potentials below the H_3^+ potential.

B. Results from the one-dimensional study

It is important to remember that in the experiment, the H^- fragments were detected and therefore it was not possible to separate the two asymptotic channels in reaction (3). However, the diabatic $^2A_1$ state with electronic configuration $1a_1(2a_1)^2$ (the "ion-pair state") that is included in the theoretical treatment dissociates into the $H_2^+ + H^-$ fragments and therefore only this reaction is studied in the theoretical model. The states relevant for the $H + H^+ + H^-$ channel are not included in the present study. Therefore, it is not possible to compare the measured and calculated cross sections for electron energies larger than 8.1 eV, where the second dissociation channel opens up.

The two-dimensional theoretical study of the ion-pair formation is much more difficult and time consuming compared to the one-dimensional model. Not only because the numerical time propagation on coupled potentials is more demanding, but also since the potential energy surfaces and couplings have to be calculated for two dimensions. Therefore, we found it convenient to investigate the influences of the couplings between the neutral H_3 states, using the one-dimensional model. The results from these tests can be seen in Fig. 6. In all these calculations, it is assumed that the ions are vibrationally relaxed when they recombine with the electron. Also autoionization from the resonant states is included. In the first calculation, only the diabatic one-dimensional ion-pair potential is included. All electronic couplings to the other neutral states are neglected. The resulting cross section is shown in Fig. 6 with a solid line. Compared with the experimental cross section, the calculated cross section is peaked at lower energies and thus also the threshold is much sharper. Also, the cross section with no couplings included is about a factor of 7.5 larger than the experimental cross section. The next step is to include the second resonant state of $^2A_1$ symmetry and the direct coupling in the Franck-Condon region between the two resonances. As can be seen by the dashed curve in the figure, the coupling between the two resonant states will induce a double-peak in the cross section that cannot be seen in the measured cross section. The magnitude of the calculated cross section is still very large. The double peak in the cross section can be explained from the fact that the two wave packets initiated on the two different resonant potential-energy curves of H_3 have different average velocities (due to the difference in the slopes of the curves) and the electronic coupling between the two resonances will make it possible for the two wave packets to

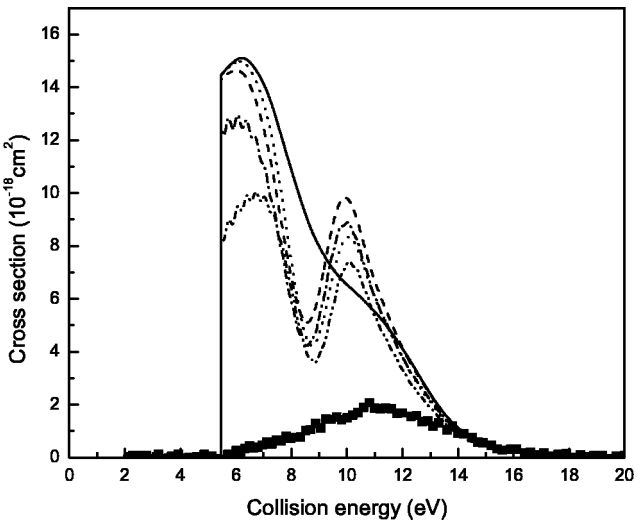

FIG. 6. Cross section of the formation of $H_2^+ + H^-$, calculated using the one-dimensional model. The solid curve is the cross section calculated by propagating a wave packet on the diabatic ion-pair state alone, without any couplings to the other neutral states. The dashed curve is obtained when direct coupling to the second resonant state is included in the calculation. The cross section shown with a dotted curve is obtained when also the indirect coupling between the two resonances is included. Finally also the couplings to the Rydberg states are included first at small internuclear distances (dashed-dotted curve) and then also at large distances (dashed-dot-dot). For comparison also the experimental cross section is included with filled squares.

interact and interfere. When all degrees of freedom are included in the model of the dynamics, interference structures in the ion-pair cross section will be smeared out. When also the indirect coupling between the two resonances is included, the ion-pair cross section changes only insignificantly as can be seen from the dotted curve in Fig. 6. In the following step, the couplings between the ion-pair state and the Rydberg states at small internuclear distances are included and as can be seen from the dashed-dotted curve, the ion-pair cross section decreases without changing the overall shape. When the electronic interaction to the Rydberg states at larger distances is included in the calculation, the ion-pair cross section drops even more.

To summarize, from the one-dimensional calculations we can conclude that the one-dimensional model cannot reproduce the position of the peak in the ion-pair cross section correctly. The peak is shifted to lower energies and therefore the threshold of the calculated cross section is too sharp. The one-dimensional resonant potential-energy curve is too low in energy in the Franck-Condon region. The couplings between the ion-pair state and the Rydberg states are important for reducing the magnitude of the cross section. By including these couplings, the cross section goes down by a factor of two. But still the peak value of the calculated cross section is about a factor of 5.2 larger than the peak value of the measured cross section. Finally, the coupling to the other resonant state will introduce a double-peak structure that cannot be seen in the experimental cross section since, in reality, the dynamics is not in one dimension.

C. Results from the two-dimensional study

We have studied the formation of the ion-pair $H_2^+ + H^-$ and it is obvious that we cannot follow the reaction path in the dynamics using the simple one-dimensional model, i.e., the H-H equilibrium bond length in H_3^+ is $R_e = 1.65a_0$, while it is $2.0a_0$ for H_2^+. From the one-dimensional model, we observed that we could not describe the electron capture correctly. The next step was to include both radial Jacobi coordinates, R and z (see Fig. 2) in the treatment of the dissociation dynamics. The results from these calculations can be seen in Fig. 7. Again, it was assumed that the ions are vibrationally relaxed and autoionization is included. In the first calculation, the two-dimensional wave packet is propagated on the ion-pair potential, without any couplings to the other states. Now, the position of the peak in the calculated cross section agrees with the measured cross section. Thus, it is necessary to include both the R and z degrees of freedom in the electron capture process. The magnitude of the calculated two-dimensional ion-pair cross section with no couplings, is about the same as the magnitude of the corresponding one-dimensional calculation. When the direct coupling between the resonant states are included, the cross section drops in magnitude and shifts to slightly lower energy. A shoulder develops in the low-energy side, due to the flux which is captured into the other state and then through coupling crosses to the diabatic ion-pair state. In the two-dimensional calculation the couplings between the two resonant states will not produce the sharp two-peak structure in the cross section observed in the one-dimensional study. The cross section is still too large in magnitude since the loss to the Rydberg states has not been included.

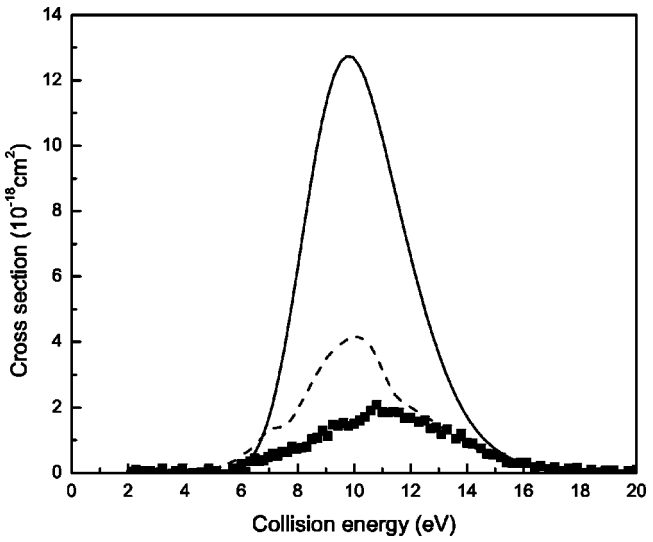

FIG. 7. Cross section of the formation of $H_2^+ + H^-$ in electron recombination with $H_3^+(v_1=0,v_2=0)$ calculated using the two-dimensional model. The solid curve shows the cross section when no coupling is included between the two resonant states of H_3. In the calculation that produces the dashed curve, both the direct and indirect couplings between these two resonant states are included. Also the experimental cross section is included with filled squares in the figure.

Another interesting property to investigate is how the ion-pair cross section changes when the H_3^+ ions are vibrationally excited. Using the two-dimensional model, on the diabatic coupled surfaces, the ion-pair cross section was calculated for ions in different vibrational states. The resulting cross section is displayed in Fig. 8. By constructing a superposition of different excited states of H_3^+ it is possible to obtain a cross section that is shifted towards lower energies and with a sharper threshold. This is also an indication that in the experiments of Yousif *et al.* [18] and Peart *et al.* [17], the ions were not vibrationally relaxed to the lowest vibrational level only. Experimental studies on the effect of the vibrational population on the DR of H_3^+ ions are published in the literature. Using imaging measurements on DR of H_3^+ [43] at low collision energies, the vibrational population of the H_2 fragments have previously been measured. A rather wide distribution was observed for the vibrational population and basically all vibrational states were populated. However, it should be noted that this measurement was carried out at low energies, where completely different states are relevant compared to the states relevant for ion-pair formation.

V. SUMMARY

In the energy regime 5–15 eV, the DR and RIP reactions of H_3^+ involves the stabilization, via fragmentation, of the same intermediate doubly excited neutral state, H_3^{**} [see Eqs. (2) and (3)]. As such, one might expect some similarity in the behavior of the cross sections and, indeed, both cross

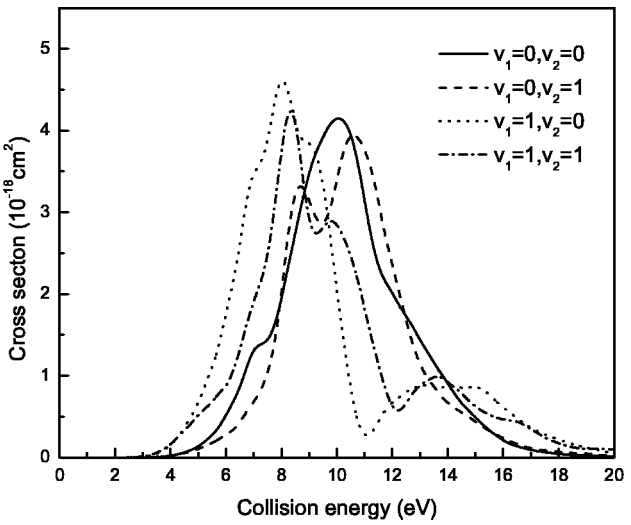

FIG. 8. Ion-pair cross section for different initial vibrational levels of the ion. It can be seen that for higher vibrational levels, the peak of the cross section shifts to lower energies and therefore it can be assumed that if all ions are not vibrationally relaxed, the threshold of the ion-pair cross section will be sharper compared with the cross section from completely vibrationally relaxed ions.

sections have a local maximum in the energy region 5–15 eV, as can be seen in Fig. 4. The position of this maximum and the energy dependence of the RIP cross section can be understood in terms of the present theoretical considerations after including both C_{2v} degrees of freedom in the initial electron capture and the dissociation dynamics. Moreover, as shown in Fig. 7, the two-dimensional treatment of dissociation dynamics clearly illustrates the importance of the couplings between the resonant states of $^2A_1$ symmetry, one of which correlates to the ion-pair limit at infinity. After including the direct coupling between these states in the Franck-Condon region, the magnitude of the calculated cross section reduces significantly, becoming only twice as large as the measured cross section.

As has been observed in our earlier studies in which the DR and RIP processes have been measured, e.g., HD^+ [20] and NO^+ [44], the magnitude of the RIP cross section is only a few percent of the total DR cross section. The only exception noted so far to this observation has been HF^+ [45], for which the RIP signal is 20% of the DR signal. These observations indicate that, for H_3^+, most of the dissociation flux progressing along the potential of the $^2A_1$ intermediate resonant state is being redirected onto a series of Rydberg states converging to the ion ground state. Indeed, this is confirmed by the present results for the one-dimensional theoretical study which show that after taking into account the couplings between the ion-pair resonant state and the Rydberg states (both at small and large internuclear distances) the cross section decreases by almost a factor of two (see Fig. 6). In order to minimize time-consuming calculations, the couplings between the resonant and the Rydberg states are not included in the present two-dimensional treatment. A full two-dimensional calculation, including the couplings both between resonant and Rydberg states is planned [42]. One can expect that the redirection of the dissociation flux to the Rydberg states will result in a similar reduction of the RIP cross section as was found in the one-dimensional model. Thus the magnitude of the measured cross section is expected to be satisfactorily reproduced in our two-dimensional treatment.

As mentioned previously, H_3^+ is a system in which the resonant ion-pair curve crosses a manifold of Rydberg states twice, both at small and large internuclear separations. It has been shown that in case of HD^+ the double crossing of the resonant ion-pair state with a series of Rydberg states leads to oscillations as a function of electron energy in the RIP cross section [20]. It might be expected that similar oscillations should be observed in the RIP of H_3^+. However, the present experimental data show no oscillations. This might be due to the extra degrees of freedom in the triatomic system which washes out the oscillations.

ACKNOWLEDGMENTS

This work is supported by the European Community's Research Training Networks Program under Contract No. HPRN-CT-2000-0142 and the Training Site Program under Contract No. HPMT-CT-2001-00226. J.S. acknowledges support in part by the State Committee for Scientific Research. Å.L. is supported from the Swedish Foundation of International Cooperation in Research and Education (STINT) and The Knut and Alice Wallenberg Foundation. N.D. and G.H.D. acknowledge support in part from the Office of Fusion Energy Sciences, Office of Basic Energy Sciences of the U.S. Department of Energy under Contract No. DE-A102-95ER54293. A.E.O. acknowledges support from the National Science Foundation, Grant No. PHY-99-87877.

[1] T.J. Miller, D.J. DeFrees, A.D. Mclean, and E. Herbst, Astron. Astrophys. **194**, 250 (1977).
[2] B.J. McCall and T. Oka, Science **287**, 1941 (2000).
[3] B.J. McCall, K. H Hinkle, T.R. Geballe, and T. Oka, Faraday Discuss. **109**, 267 (1998).
[4] B.J. McCall, T.R. Geballe, K.H. Hinkle, and T. Oka, Science **279**, 1910 (1998).
[5] E. Herbst and W. Klemperer, Astrophys. J. **185**, 505 (1973).
[6] D.W. Martin, E.W. McDaniel, and M.L. Meeks, Astrophys. J. **183**, 112 (1961).
[7] M. Larsson, H. Danared, J.R. Mowat, P. Sigray, G. Sundström, L. Bostrom, A. Filevich, A. Källberg, S. Mannervik, K.G. Rensfeldt, and S. Datz, Phys. Rev. Lett. **70**, 430 (1993).
[8] M. Larsson, H. Danared, Å. Larson, A. Le Padellec, J.R. Peterson, S. Rosén, J. Semaniak, and C. Strömholm, Phys. Rev. Lett. **79**, 395 (1997).
[9] M. Larsson, Philos. Trans. R. Soc. London, Ser. A **358**, 2433 (2000).
[10] M.J. Jensen, H.B. Pedersen, C.P. Safvan, K. Seiersen, X. Urbain, and L.H. Andersen, Phys. Rev. A **63**, 052701 (2001).

[11] H. Kreckel, S. Krohn, L. Lammich, M. Lange, J. Levin, M. Scheffel, D. Schwalm, J. Tennyson, Z. Vager, R. Wester, A. Wolf, and D. Zajfman, Phys. Rev. A **66**, 052509 (2002).
[12] M. Larsson, N. Djurić, G.H. Dunn, A. Neau, A.M. Derkatch, F. Hellberg, S. Kalhori, D.B. Popović, J. Semaniak, Å. Larson, and R. Thomas, in *Proceedings on the Symposium on Dissociative Recombination*, American Chemical Society, edited by S. Guberman (Kluwer Academic/Plenum, New York, 2003), p. 87.
[13] B.J. McCall, A.J. Huneycutt, R.J. Saykally, T.R. Gebale, N. Djurić, G.H. Dunn, J. Semaniak, O. Novotny, A. Al-Khalili, A. Ehlerding, F. Hellberg, S. Kalhori, A. Neau, R. Thomas, F. Österdahl, and M. Larsson, Nature (London) **422**, 500 (2003).
[14] V. Kokoouline, C.H. Greene, and B.D. Esry, Nature (London) **412**, 891 (2001).
[15] V. Kokoouline and C.H. Greene, Phys. Rev. Lett. **90**, 133201 (2003).
[16] http://webbook.nist.gov/
[17] B. Peart, R.A. Forrest, and K.T. Dolder, J. Phys. B **12**, 3441 (1979).
[18] F.B. Yousif, P. Van der Donk, and J.B.A. Mitchell, J. Phys. B **26**, 4249 (1993).
[19] Å. Larson and A.E. Orel, Phys. Rev. A **59**, 3601 (1999).
[20] Å. Larson, N. Djurić, W. Zong, C.H. Greene, A.E. Orel, A. Al-Khalili, A.M. Derkatch, A. Le Padellec, A. Neau, S. Rosén, W. Shi, L. Vikor, H. Danared, M. af Ugglas, M. Larsson, and G.H. Dunn, Phys. Rev. A **62**, 042707 (2000).
[21] M.B. Någård, J.B.C. Pettersson, A.M. Derkatch, A. Al-Khalili, A. Neau, S. Rosén, M. Larsson, J. Semaniak, H. Danared, A. Källberg, F. Österdahl, and M. af Ugglas, J. Chem. Phys. **117**, 5264 (2002).
[22] A. Neau, A. Al-Khalili, S. Rosén, A. Le Padellec, A.M. Derkatch, W. Shi, L. Vikor, M. Larsson, R. Thomas, M.B. Någård, K. Andersson, H. Danared, and M. af Ugglas, J. Chem. Phys. **113**, 1762 (2000).
[23] B.J. McCall *et al.* (unpublished).
[24] G. Kilgus, D. Habs, D. Schwalm, A. Wolf, N.R. Badnell, and A. Müller, Phys. Rev. A **46**, 5730 (1992).
[25] D.R. DeWitt, R. Schuch, T. Quinteros, H. Gao, W. Zong, H. Danared, M. Pajek, and N.R. Badnell, Phys. Rev. A **50**, 1257 (1994).
[26] A. Lampert, A. Wolf, D. Habs, J. Kettner, G. Kilgus, D. Schwalm, M.S. Pindzola, and N.R. Badnell, Phys. Rev. A **53**, 1413 (1996).
[27] H. Danared (private communication).
[28] A.E. Orel and K.C. Kulander, Phys. Rev. Lett. **71**, 4315 (1993).
[29] A.E. Orel, K.C. Kulander, and B.H. Lengsfield III, J. Chem. Phys. **100**, 1756 (1994).
[30] H.H. Michels and R.H. Hobbs, Astrophys. J. **286**, L27 (1984).
[31] D.R. Bates and J.T. Lewis, Proc. R. Soc. London, Ser. A **68**, 173 (1955).
[32] K.C. Kulander and M.F. Guest, J. Phys. B **12**, L501 (1979).
[33] Å. Larson and A.E. Orel, Phys. Rev. A **64**, 062701 (2001).
[34] A. Giusti-Suzor, J.N. Bardsley, and C. Derkits, Phys. Rev. A **28**, 682 (1983).
[35] H. Estrada, L.S. Cederbaum, and W. Domcke, J. Chem. Phys. **84**, 152 (1986).
[36] A.U. Hazi, J. Phys. B **16**, L29 (1983).
[37] J. Royal, Å. Larson, and A.E. Orel (unpublished).
[38] A. Goldberg, H.M. Schev, and J. Schwartz, Am. J. Phys. **35**, 177 (1967).
[39] D.G. Truhlar, J. Comput. Phys. **10**, 123 (1972).
[40] H. Tal-Ezer and R. Kosloff, J. Chem. Phys. **81**, 3967 (1984).
[41] I.F. Schneider and A.E. Orel, J. Chem. Phys. **111**, 5873 (1999).
[42] A.E. Orel and Å. Larson (private communication).
[43] D. Strasser, L. Lammich, H. Kreckel, S. Krohn, M. Lange, A. Naaman, D. Schwalm, A. Wolf, and D. Zajfman, Phys. Rev. A **66**, 032719 (2002).
[44] A. Le Padellec, N. Djurić, A. Al-Khalili, H. Danared, A.M. Derkatch, A. Neau, D.B. Popović, S. Rosén, J. Semaniak, R. Thomas, M. af Ugglas, W. Zong, and M. Larsson, Phys. Rev. A **64**, 012702 (2001).
[45] N. Djurić, A. Al-Khalili, A.M. Derkatch, A. Neau, S. Rosén, W. Shi, L. Vikor, W. Zong, A. Le Padellec, H. Danared, M. af Ugglas, M. Larsson, and G.H. Dunn, Phys. Rev. A **64**, 022713 (2001).